Proceedings of ENCIT 2010
13th Brazilian Congress of Thermal Sciences and Engineering
December 05-10, 2010, Uberlandia, MG, Brazil

OPTIMIZATION OF ABSORBING BOUNDARY METHODS FOR ACOUSTIC WAVE MODELLING

Roger Matsumoto Moreira [1,3,4], roger@vm.uff.br
Raul Bernardo Vidal Pessolani [2], raul@vm.uff.br
Elkin F. Rodriguez Velandia [1,3], elkinrodvel@msn.com
Theo Dias Kassuga [1], theodk@gmail.com
[1] LabCFD, [2] TEM, [3] PGMEC & [4] PGEQ / School of Engineering / Fluminense Federal University
Rua Passos da Pátria 156, bl.D, Niterói, RJ, Brazil. CEP: 24210-240.

André Bulcão, bulcao@petrobras.com.br
CENPES / PETROBRAS
Cidade Universitária, Ilha do Fundão, RJ, Brazil.

Abstract. *This work aims to perform effectiveness tests for optimized nonreflecting boundary conditions in a finite difference time domain (FDTD) scheme applied to acoustic wave modelling. Our goal is to enhance the classical absorbing boundary methods – namely Absorbing Boundary Condition (ABC), Damping Zone (DZ) and Perfect Matched Layer (PML) – in order to minimize the spurious reflections associated with, improving the quality of the numerical results and reducing its computational effort. ABC, PML and DZ methods are presented and optimized aiming to reduce wave reflection at the borders, with results shown in terms of the total energy for "infinite" and nonreflecting models for varying absorbing layers. It has been found that both optimizations increase the effectiveness of the absorbing layer, with better absorption efficiencies for the optimized Cerjan and PML methods. Results also show that side effects are very sensitive to the number of grid points used in the absorbing layer, with better results found for larger discretization points.*

Keywords*: acoustics, absorbing boundary condition, finite difference method.*

1. INTRODUCTION

The appearance of fast processing computers and the continuous advances in numerical analysis have allowed new developments in acoustic wave modelling. For imaging the subsurface, many articles have been published dealing with numerical simulations of wave propagation using finite difference, finite element and boundary integral methods (Virieux 1986, Marfurt 1984, Schuster 1985, Durran 1999). A typical difficulty that arises when solving numerically such boundary value problems is how to express the radiation condition mathematically at a contour which is only at a finite distance from the energy source (Sommerfeld 1949). The boundary condition should allow travelling disturbances to pass through the contour without generating spurious reflections that propagate back toward the interior, which may eventually override the original emitted seismic signals.

To avoid these side effects, researchers used to enlarge the computational domain, delaying the backward reflections, though increasing the numerical mesh and its computational demand. In the late 70's, nonreflecting boundary condition techniques were introduced aiming to treat such problems. Clayton and Engquist (1977) proposed the Absorbing Boundary Condition (ABC) technique by applying a one-way wave equation in the boundary region, which proved to be efficient for events not at shallow angles on the contour. In the early 80's, Cerjan *et al.* (1985) introduced the Damping Zone (DZ) concept in which a gradual reduction of the wave amplitude is imposed along an absorption layer, without any loss of effectiveness due to shallow angles of wave incidence. More recently, Berenger (1994) proposed the Perfect Matched Layer (PML) method for solving electromagnetic and elastic wave equations. A new matched medium is designed to absorb without reflection the incident waves at any frequency and at any incidence angle.

This article presents numerical simulations obtained via a 10^{th} order in space and 4^{th} order in time staggered-grid finite difference scheme applied to acoustic waves. Figure 1 exemplifies the wave propagation domain with its absorbing boundary layers. Our main motivation is to reduce the number of grid points at the absorbing boundary layer for the least reflected waves inside the medium. Our goal is to enhance the existing absorbing boundary methods in order to minimize the errors associated with, improving the quality of the numerical results and reducing its computational effort. First, DZ, PML and ABC methods are presented and optimized aiming to reduce wave reflection at the borders, with results shown in terms of the total energy for "infinite" and nonreflecting models for varying absorbing layers.

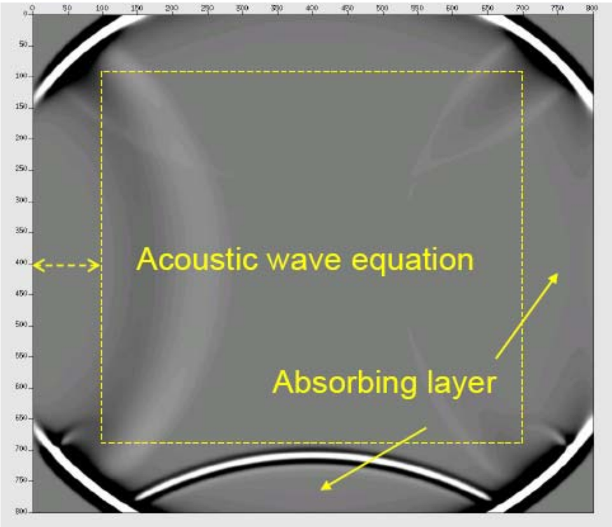

Figure 1. Wave propagation domain with absorbing boundary layers.

2. PML METHOD

2.1. Conventional PML

When the disturbances generated by a source reach the limits of the computational domain, reflected waves are spread throughout the medium. To avoid this problem, Berenger (1994) developed the PML technique, in which a new region that surrounds the FDTD is defined, where a set of non-physical equations are applied giving a high attenuation of the incident waves.

For acoustics, the 2D linearized continuity and Euler equations take the following form at the PML absorbing layer,

$$p_t + B\alpha p = -B\nabla \cdot \vec{u}\ , \tag{1}$$

$$\vec{u}_t + B\alpha\vec{u} = -\frac{1}{\rho}\nabla p\ , \tag{2}$$

where ρ, p and $\vec{u}$ are, respectively, the medium density and the acoustics' pressure and velocity, while α is the attenuation coefficient and B ($= \rho c^2$) the medium bulk modulus. c is the medium wave speed.

Differentiating in time and space equations (1) and (2) and subtracting the resulting expressions give the PML acoustic equation,

$$p_{tt} + \alpha(1+B)p_t + \alpha^2 Bp = c^2\nabla^2 p\ . \tag{3}$$

The conventional attenuation coefficient α varies accordingly to,

$$\alpha(i) = \frac{1}{B\delta t}\ln\left(\frac{1}{r_{PML}}\right)\left[\frac{x(i)}{x(n_{PML})}\right]^k , \tag{4}$$

in which the maximum applied absorption rate r_{PML} is equal to 1/10 and the exponent k=2. Therefore α oscillates from 0 (when x is at the border of the absorbing layer, thus satisfying the acoustic wave equation) to $ln(10)/(B\delta t)$, where δt is the time step and n_{PML} the number of PML grid elements. The integer i represents the grid element such that $1 \le i \le n_{PML}$.

2.2. Optimized PML

In a general form, α can be rewritten as,

$$\alpha(i) = c_{PML} f[x(i)]. \tag{5}$$

Changing the values of c_{PML} and the function $f[x(i)]$, for a fixed n_{PML}, improves the effectiveness of the absorption, reducing its side effects by increasing the absorption rate and using smoother polynomials at the absorbing layer. Figure 2 shows some of the tested attenuation functions $f[x(i)]$ for n_{PML}=20.

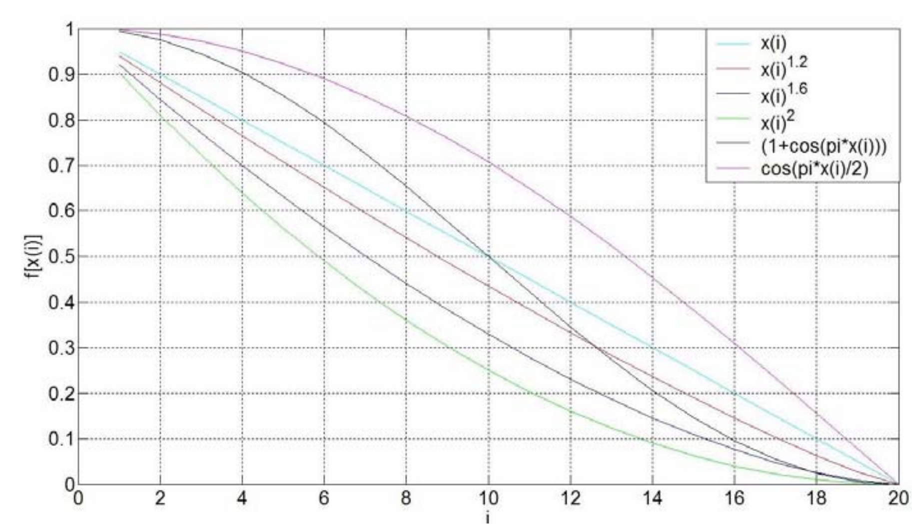

Figure 2. Tested attenuation functions $f[x(i)]$ for the optimized PML method.

3. DZ TECHNIQUE

3.1. Conventional Cerjan

The DZ technique – originally proposed by Cerjan *et al.* (1986) – introduces a damping zone around the domain consisting of *Na* points, where the wave amplitude is absorbed by the relation,

$$Fac = e^{-(factor*(Na-i))^2} \quad . \tag{6}$$

where the original coefficient *factor* is 0,015 for *Na* points in the damping layer and *i* varies from 1 to *Na*. The factor remains constant throughout the boundary absorbing layer.

The wave amplitude gradually diminishes, but at the end of the process a small amount of energy is reflected. For a more accurate analysis, this reflection cannot be accepted. To minimize the reflected energy, a common procedure is to increase the number of points in the damping layer. At first reflection decreases, but from a certain number of points it tends to remain constant. A procedure to minimize the reflected energy was then developed to try to reduce that error.

3.2. Optimized Cerjan: varying coefficient factors

In order to try to improve the conventional Cerjan's method, the coefficient factors are calculated varying the number of points from 20 to 100 at the boundary layer and computing the total reflected energy by the squared amplitude difference at each time step, between the model with an "infinite" domain and with the artificial boundary. The computed factors are shown in figure 3.

3.3. Optimized Cerjan: velocity reducer

A second way for optimizing Cerjan's technique is to couple a coefficient factor that reduces the wave velocity propagation. It was verified that Cerjan's coefficient factor works better for low velocities. Therefore the acoustic wave equation can be rewritten as,

$$p_{tt} = c^2 FRv^2 \nabla^2 p \; . \tag{7}$$

The factor *FRv* follows a quadratic form,

$$FRv = \frac{(1-Fv)}{Na^2} x^2 - 2\frac{(1-Fv)}{Na} x + 1 \tag{8}$$

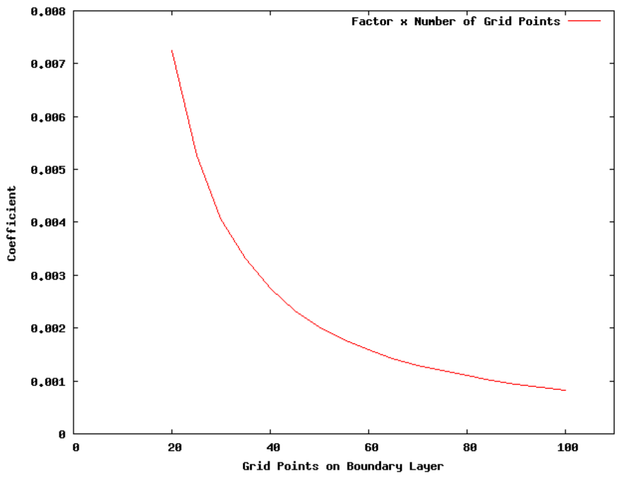

Figure 3. Coefficient factors as a function of the number of grid points for the optimized Cerjan's method.

where *FRv* varies from 1 (when $x=Na$) to *Fv* (when $x=1$).

4. ABC METHOD

4.1. Conventional ABC

The ABC technique – originally proposed by Clayton and Engquist (1977) – transforms the boundary conditions in order to minimize artificial reflections. The new boundary conditions are based on paraxial approximations of the wave equation, which is an extrapolation of the wave-field inside the domain. An approximation of first order is given by:

$$\frac{\partial U}{\partial z} + \frac{1}{v}\frac{\partial U}{\partial t} = 0 \cdot \tag{9}$$

U is the wave amplitude and v the wave speed. This procedure will be tested with other techniques as described below.

4.2. ABC with Liu technique

In order to minimize the waves that are coming to the boundary providing a smooth variation, Liu and Sem (2010) proposed to insert a transition area between the domain and the boundary. They divided the whole domain into three blocks (see figure 4): an inner area (I), the transition (II) and the boundary (III). The wave field within the inner area is computed using the wave equation, while into the transition area it is computed by the wave equation and the one-way equation. The final wave field into area II is found by applying a weighted average between the two values, given by:

$$U_2 = (1-w)U_1 + w.U_3 \tag{10}$$

where w is the weight factor varying linearly from 1 to zero in ten points of the area II. This procedure provides a smooth variation from area I to area III. In area III, the wave field is calculated by the conventional ABC extrapolation.

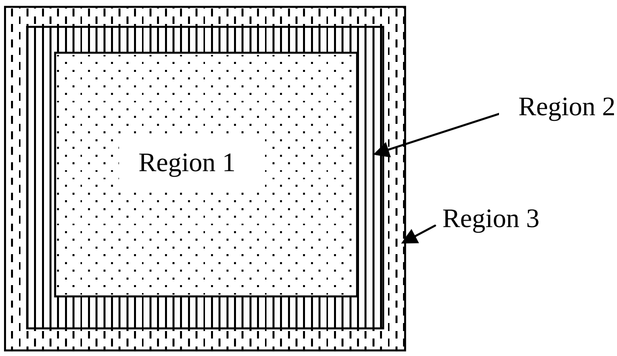

Figure 4. The three regions of Liu´s method.

5. METHODOLOGY

The effectiveness of the three different algorithms of wave absorption in the boundary layer was compared. For all algorithms, absorption layers with different thickness were tested. At time *t=0*, a Ricker type source is generated at the center of the model with waves propagating through a finite difference method. As an energy measure, the square of the amplitude over the whole domain was taken to evaluate the effectiveness of each absorption boundary,

$$E_{Effectiveness} = \sum (U)^2 . \tag{6}$$

The model used was a 2D constant velocity (3000 m/s) grid. As shown in Figure 5, the region without the absorption layer (Region 1) has 601x601 grid points. Around this region, a boundary layer was created with thickness varying from 20 to 150 grid points. The wave absorption algorithms were applied in these boundary layers. The finite difference operator used is of 4th order in time and 10th order in space. To avoid instability and divergence problems with the numerical method, the grid spacing used is of 5m and the time step 0,0002s. The distance between the source and the receiver is of 294 grid points or 1470m.

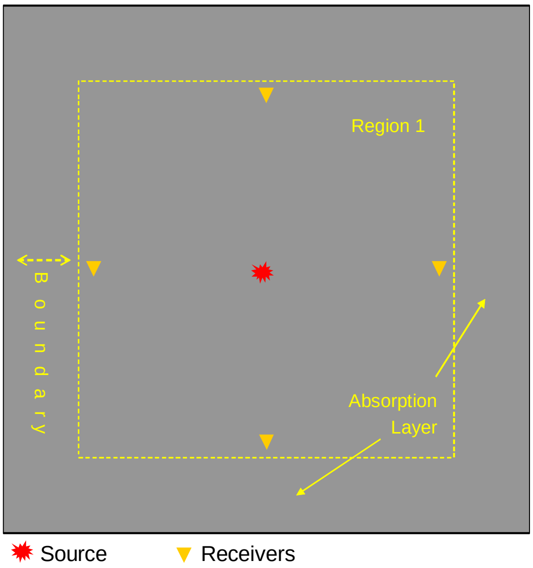

Figure 5. Wave propagation domain with absorbing boundary conditions.

6. RESULTS

6.1. PML

Figure 6 compares the effectiveness of wave absorption for the original (PML2-10: k=2, r_{PML}=1/10) and optimized PML methods (PML5-10: k=5, r_{PML}=1/10; PML2-1.1: k=2, r_{PML}=9/10; PML5-1.1: k=5, r_{PML}=9/10; PML7-10: k=7, r_{PML}=1/10) with varying absorbing layers. Results show that, for a small number of PML grid elements ($n_{PML}=25, 50$), the application of larger maximum absorption rates (r_{PML}=9/10) proves to be more efficient to absorb incident waves, reducing significantly wave reflections at the border.

On the other hand, for larger PML layers ($n_{PML}=75, 100, 150$), a conjugated use of maximum absorption rates (r_{PML}=9/10) and higher order polynomials (k=5, 7) improve the effectiveness of the absorbing layer. In fact, figure 7 illustrates that the proposed optimized PML models are more effective than the original's Cerjan and PML methods.

As explained in section 2.2, further investigations reveal that better absorption rates can be found for certain values of c_{PML} and functions $f[x(i)]$. Figure 8 shows that a quadratic function for the attenuation function $f[x(i)]$ with c_{PML}=3,55 x 10^{-8} gives the minimum reflection for n_{PML}=20, which represents less than 0,5% of the total incident wave energy. Other functions were also tested which proved to be more efficient absorbers when compared to the original PML method.

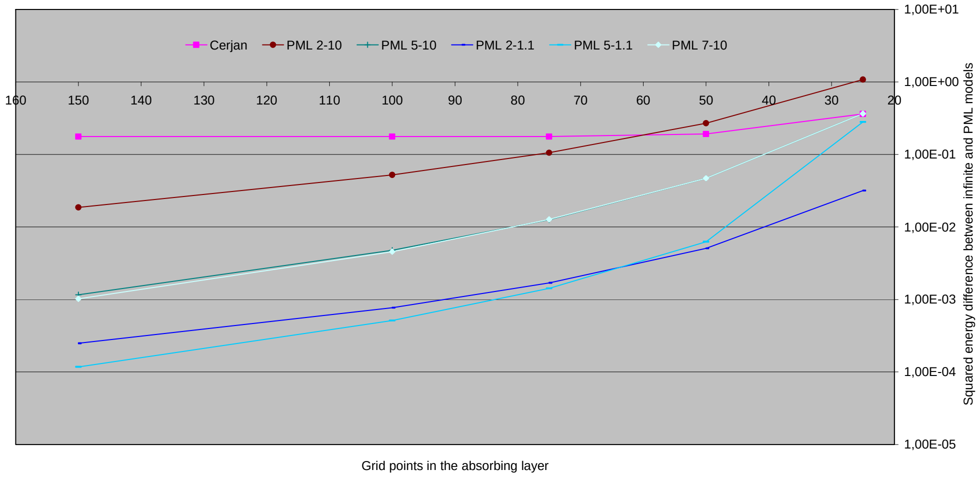

Figure 6. Time sum of squared energy difference between “infinite” and nonreflecting boundary methods for varying absorbing layers.

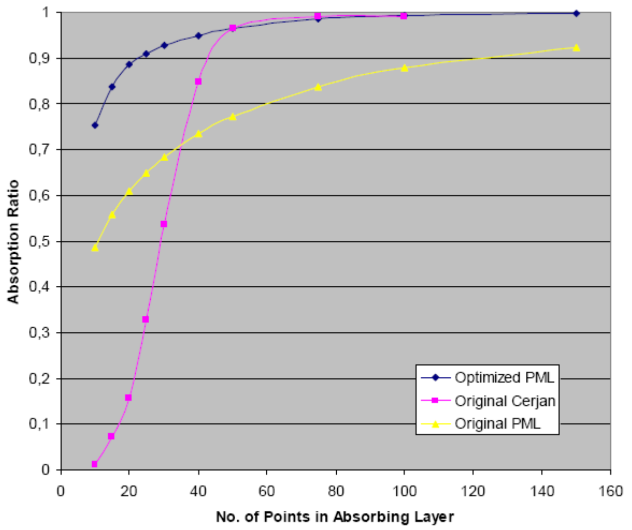

Figure 7. Energy absorption ratio between infinite and nonreflecting boundary methods for varying absorbing layers.

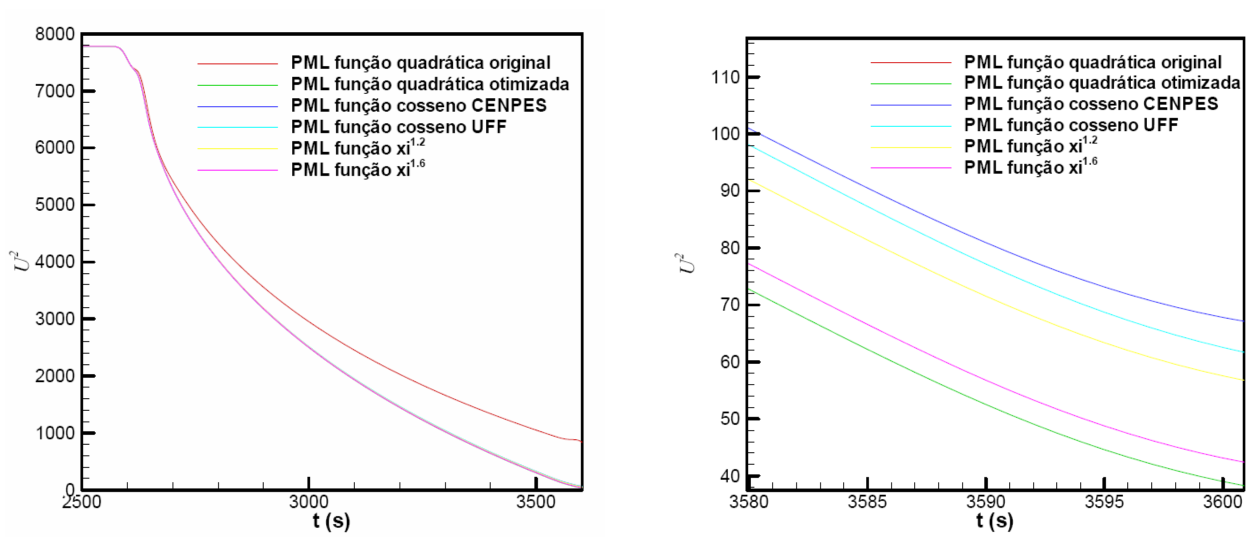

(a) (b)

Figure 8. Optimized PML: total reflected energy for different attenuation functions $f[x(i)]$.

6.2. DZ

Figure 9 shows the amount of energy reflection and the number of boundary points. It shows a comparison between the original Cerjan's method and its optimization by varying the coefficient factors. It can be seen that the original Cerjan's curve is constant after 25 grid points at the boundary layer, while in the optimized one, the error decreases with the number of grid points at the boundary layer. The main goal is to develop a method that minimize the error and do not increase the computational effort. The use of a velocity reducer also proves to be very efficient with a reduction of the wave energy reflection in almost 60% compared to the standard Cerjan method, for boundary layers until 50 points, which is shown in figure 10.

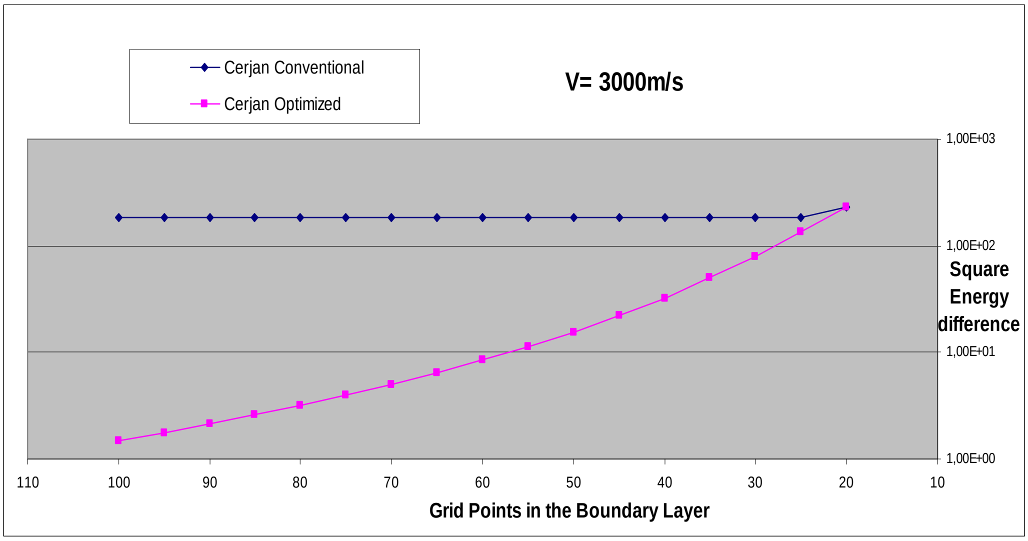

Figure 9. Comparison between Cerjan's conventional and optimized methods.

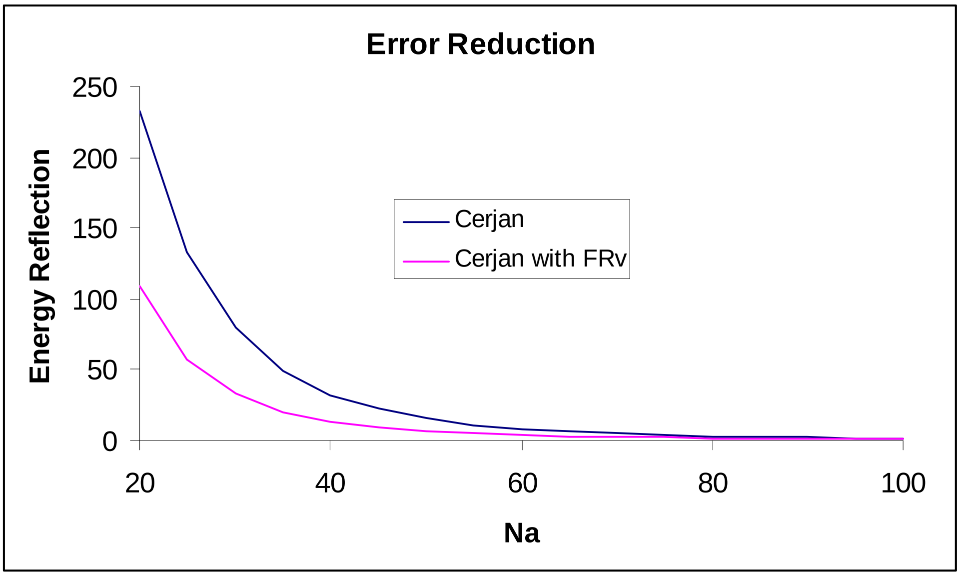

Figure 10. Energy reflection using the velocity reduction factor.

6.3. ABC and hybrid techniques

These techniques have their results compared. In the first example (see figure 11), a source with 5,64 Hz was used and the techniques of ABC, ABC + Liu, Cerjan Optimized with 20 layer points, and the combination ABC+Liu+Cerjan were applied. Notice that Cerjan had a worse performance compared to other techniques, which practically reduced to zero emission energy. The absorber ABC and ABC + Liu worked better than the combination with the Cerjan absorber. Table 1 shows the absorbing rates for various methods.

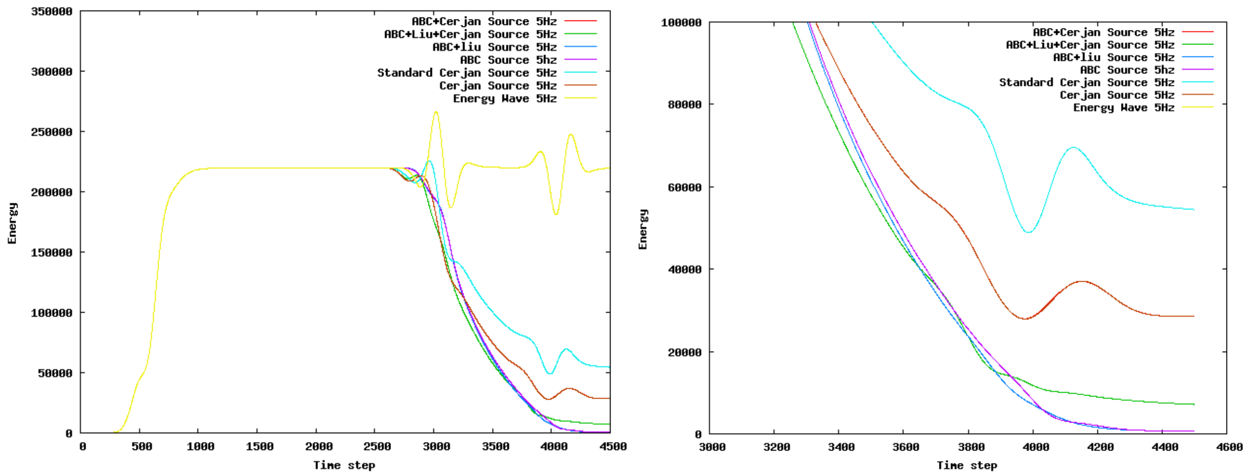

(a) (b)

Figure 11. Energy of the various absorbing methods with a source of 5Hz and a detail.

Table 1. Absorbing tax for a source of 5Hz.

Case 5Hz	Final Energy	Absorbing Rate
Without Absorber	219458	0%
ABC	618	99,72%
ABC+Liu	601	99,73%
Standard Cerjan	54434	75,2%
Cerjan Optimized	28529	87,00%
ABC+Cerjan	28544	87,00%
ABC+Liu+Cerjan	7538	96,56%

In a second example, the frequency was increased to 30Hz and results are shown in figure 12. Note that the optimized Cerjan improved considerably, but the absorption of ABC+Liu was better. Table 2 shows that the efficiency of the absorbers depends on the frequency of the source. Finally figure 13 shows the computed CPU time for each method.

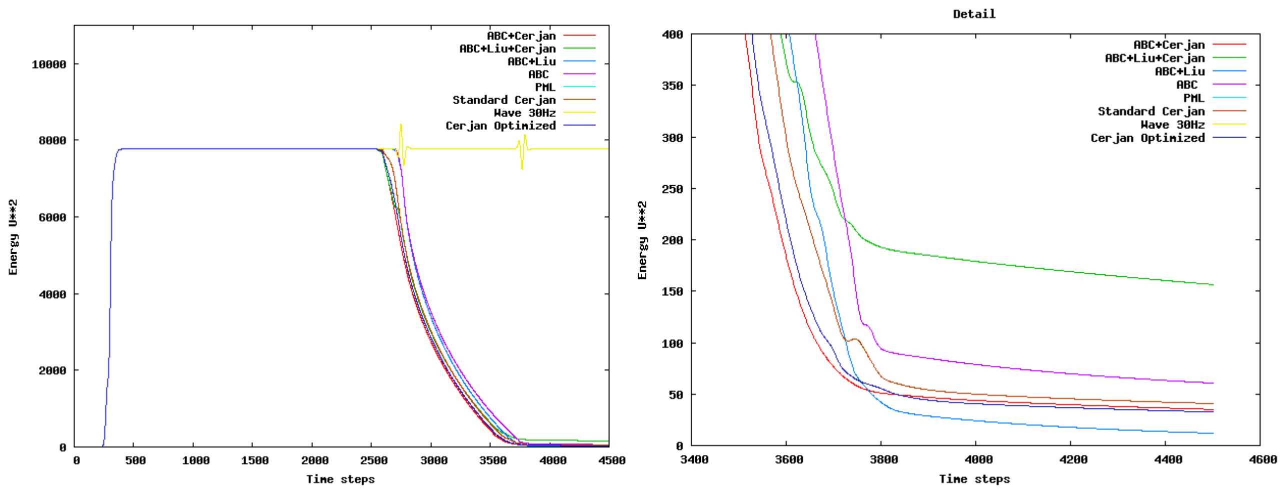

(a) (b)

Figure 12. Energy of the various absorbing methods with a source of 30Hz and a detail.

Table 2. Absorbing tax for a source of 30Hz.

Case 30Hz	Final Energy	Absorbing Tax
Without Absorber	7752	0%
ABC	60,61	99,21%
ABC+Liu	11,96	99,84%
Standard Cerjan	40,81	99,47%
Cerjan Optimized	32,59	99,57%
ABC+Cerjan	35,06	99,54%
ABC+Liu+Cerjan	156,39	97,98%
PML	33,84	99,56%

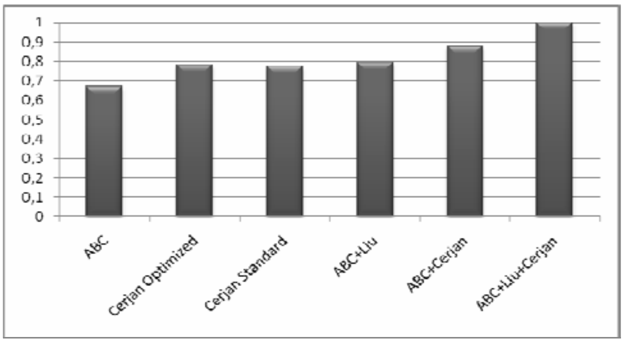

Figure 13. CPU time for various methods.

7. CONCLUSIONS

Some classical nonreflecting boundary methods – PML, DZ and ABC – were optimized aiming to reduce wave reflections at the borders of the FDTD 2D computational domain. It has been found that optimizations increase the effectiveness of the absorbing layer, with better absorption efficiencies for the optimized Cerjan and PML methods. Results also show that side effects are very sensitive to the number of grid points used in the absorbing layer, with better results found for larger discretization points. Hybrid alternatives are also tested. The corresponding absorbing factors are optimized again and results are presented in terms of the number of boundary layer points, CPU time and the total energy of the system.

8. ACKNOWLEDGEMENTS

The authors from Fluminense Federal University acknowledge the financial support through PETROBRAS (contract number 0050.0042413.08.4).

9. REFERENCES

Berenger, J.-P., 1994, “A Perfectly Matched Layer for the Absorption of Electromagnetic Waves”, J. Comp. Phys., v.114, pp.185-200.

Cerjan, C., Kosloff, D., Kosloff, R. and Reshef, M., 1985, “A nonreflecting boundary condition for discrete acoustic and elastic wave equation”, Geophysics, 50, 705-708.

Clayton, R. and Engquist, B., 1977, “Absorbing boundary conditions for acoustic and elastic wave equation”, Bull. Seis. Am., v.67, pp.1529-1540.

Durran, D.R., 1999, “Numerical Methods for Wave Equations in Geophysical Fluid Dynamics”, New York: Springer-Verlag.

Liu, Y. and Mrinal, K. S., 2010, “A hybrid scheme for absorbing edge reflections in numerical modeling of wave propagation”, Geophysics, v.75.

Marfurt K, 1984, “Accuracy of finite-difference and finite-element modeling of the scalar and elastic wave equations”, Geophysics, v.49, pp.533-549.

Reynolds, A.C., 1978, “Boundary conditions for the numerical solution of wave propagation problems”, Geophysics, v.43, pp.1099-1110.

Schuster, G.T., 1985, “A hybrid BIE + Born series modeling scheme: General Born series”, Jour. of Acoustic Soc. of Am., v.77, pp.865-879.

Sommerfeld, A., 1949, "Partial Differential Equations in Physics", New York: Academic Press.

Virieux, J., 1986, "P-SV wave propagation in heterogeneous media: Velocity-stress finite-difference method", Geophysics, v.51, pp.889-901.

10. RESPONSIBILITY NOTICE

The authors are the only responsible for the printed material included in this paper.